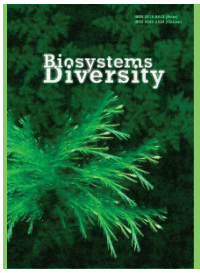

Biosystems Diversity

ISSN 2519-8513 (Print)
ISSN 2520-2529 (Online)
Biosyst. Divers.,
2024, 32(4), 407–415
doi: 10.15421/012444

Spatial and temporal variation of the rainfall erosivity factor in Polissya and Forest-Steppe of Ukraine

Y. Nykytiuk*, O. Kravchenko**, O. Komorna****, V. Bambura***, D. Seredniak*****

*Polissia National University, Zhytomyr, Ukraine
**Institute of Animals Breeding and Genetics nd. a. M. V. Zubets National Academy of Agrarian Sciences of Ukraine
***Kyiv Agrarian University of the National Academy of Agrarian Sciences, Kyiv, Ukraine
****The Institute of Innovative Education of KNUCA, Kyiv, Ukraine
*****Institute of Plant Protection of National Academy of Agrarian Sciences of Ukraine, Kyiv, Ukraine

Article info
Received 02.08.2024
Received in revised form 11.09.2024
Accepted 15.10.2024

Polissia National University, Staryi Boulevard, 7, Zhytomyr, 10008, Ukraine. Tel.: +380-67-448-38-48. E-mail: andreyniks2@gmail.com

Kyiv Agrarian University of the National Academy of Agrarian Sciences, Vasylkivska st., 37, Kyiv, 03022, Ukraine. Tel.: +380-67-135-43-80. E-mail: oksana.kravchenko@kaunaas.com

Institute of Animals Breeding and Genetics nd. a. M. V. Zubets National Academy of Agrarian Sciences of Ukraine, Pogrebnyaka st., 1, Chubynske village, 08321, Kyiv region, Ukraine. Tel.: +38-044-370-87-40. E-mail: kravchenko.irgt@gmail.com

The Institute of Innovative Education of KNUCA, Osvity st., 4, Kyiv, 03037, Ukraine. Tel.: +380-67-321-62-45. E-mail: oksanakkom@gmail.com

Institute of Plant Protection of National Academy of Agrarian Sciences of Ukraine, Vasylkivska st., 33[Kyiv, 03022, Ukraine. Tel.: +38-067-367-07-07. E-mail: d.serednyak@propecs.ua

Nykytiuk, Y., Kravchenko, O., Komorna, O., Bambura, V., & Seredniak, D. (2024). Spatial and temporal variation of the rainfall erosivity factor in Polissya and Forest-Steppe of Ukraine. Biosystems Diversity, 32(4), 407–415. doi:10.15421/012444

The Polissya and the Forest-Steppe constitute a substantial portion of Ukraine's territory, exhibiting considerable potential for the advancement of agricultural and forestry activities. It is of the utmost importance that the economic utilisation of the territory is conducted in a manner that ensures the sustainability of ecological systems and the fulfilment of ecosystem functions. The question of how the dynamics of the erosion potential of precipitation affect crop yields at the regional level remains unanswered. This study identifies patterns of spatial and temporal variability in the erosion potential of precipitation and determines the impact of anthropogenic landscape modification due to agricultural production on soil erosion risks. The coefficient of atmospheric erosion exhibited a range of 179.9 ± 114.7 (in 2015) to 616.0 ± 468.9 (in 1974) MJ mm/ha h per year. The temporal dynamics of this indicator within each administrative district exhibited a positive or negative trend of change over time. The overall level of erosion from precipitation exhibited an upward trend in the western and northwestern regions of the study area. In the central and eastern regions of the study area, there is evidence of a decline in erosion over time. The spatially weighted principal components analysis postulates that the covariance structure varies in a spatial manner, thereby enabling the identification of areas with smaller spatial coverage where the structure is constant. The identified principal components indicate the presence of oscillating time trends, characterised by different frequency characteristics. The spatial characteristics of the principal components of higher-order numbers can be attributed to the influence of the geographical continentality factor. Polissya is distinguished by soils with a relatively high sand content, which frequently renders them unsuitable for agricultural use. Consequently, these regions exhibit a relatively high level of forest cover. The southern and eastern regions are distinguished by soil types with granulometric compositions that are conducive to agricultural productivity. This frequently coincides with the process of deforestation. The variations in precipitation that generate the patterns identified by principal components 3–5 can be attributed to the influence of different land cover types. This provides an explanation for the formation of patterns of variability in the rainfall erosion coefficient, which is consistent with the level of forest cover. The influence of coniferous vegetation gives rise to the emergence of factor 4, whereas factor 5 is induced by the influence of herbaceous vegetation. It is also crucial to consider the substantial impact of agricultural land on the formation of spatial patterns of erosion coefficient variability. This influence may be the result of a formal correlation between the variability of agricultural land in different biogeographic zones.

Keywords: climate change; spatial pattern; temporal dynamic; landscape; soil cover.

Introduction

Soil erosion represents a significant environmental challenge, emerging as a consequence of agricultural intensification, land degradation, and other anthropogenic activities (Yakovenko et al., 2023). The process of water erosion involves three principal physical elements: soil, water, and plants. In light of this, three independent variables were identified as exerting control over the erosion process: soil erodibility, potential erodibility, and the protective capacity of the cover (Cook, 1937; Pandey et al., 2021). A variety of methods exist that are based on different factors, including land use, soil quality, and topography, among others, for the assessment of a region's vulnerability to soil loss. RUSLE is the most widely utilised method globally for forecasting long-term erosion rates, encompassing the scale of an individual field and extending to the spatial level of a geographic area (Wischmeier & Smith, 1978). The fundamental premise of RUSLE is that the processes of delamination and deposition are contingent upon the sedimentary composition of the flow (Zerihun et al., 2018).

The extent of erosion is not contingent on the source of the material being eroded; rather, the rate of erosion is dependent on the flow capacity (Ganasri & Ramesh, 2016). Once the sediment load reaches the flow-carrying capacity, delamination is no longer possible. Furthermore, sedimentation must also occur during the recession phase of the hydrograph, as the flow velocity decreases. The rainfall erosivity factor (R) in the RUSLE water erosion model is a measure of the impact of rainfall intensity on soil erosion. In order to calculate this factor, it is necessary to have access to detailed, continuous rainfall data (Wischmeier & Smith, 1978; Zerihun et al., 2018). R is an indicator of the two most significant characteristics of a storm that determine its erosive potential (Ganasri & Ramesh, 2016). Specifically, the focus is on the amount of precipitation and the peak intensity that persist over an extended period of time (Gámez-Balmaceda et al., 2020). A number of studies have demonstrated a direct correlation between soil loss from cultivated fields and the kinetic energy and intensity of precipitation (Majewski & Szpikowski, 2024). The rainfall erosivity factor used in RUSLE quantifies the impact of droplet impact (Nearing et al., 2017), and also reflects the amount and rate of runoff that can be associated with precipitation (Dash & Maity, 2023).

The forecasting of future changes in soil erosion is contingent upon the modelling of prospective rainfall erosion, alterations in land use, and

the influence of policies on soil loss (Panagos et al., 2017). It seems probable that the ongoing and projected climate change will affect soil erosion through a number of different mechanisms, including increased rainfall, changes in precipitation, changes in humidity, and changes in vegetation cover (Christensen et al., 2015). A rise in precipitation intensity, particularly the occurrence of greater numbers of extreme precipitation events, is expected to have the most significant impact of climate change on soil erosion (Westra et al., 2014). The greatest impact on the future will result from changes in the erosive power of rainfall (Nearing, 2001). The current generation of global climate models lacks the capacity to directly calculate the R-factor as a function of precipitation intensity and energy. In order to predict changes in the R-factor based on a global climate model, statistical relationships between monthly and annual precipitation and rainfall-induced erosion must be employed (Renard & Freimund, 1994). Based on the projected impact of rainfall on soil erosion alone, the future climate change scenario for 2100 indicates an anticipated average increase of 20% in soil erosion on agricultural land in Japan (Shiono et al., 2013).

The Polissya and Forest-Steppe regions represent a substantial portion of Ukraine's territory, exhibiting considerable potential for the advancement of agricultural and forestry activities (Zymaroieva et al., 2021). It is of the utmost importance that the active economic utilisation of the territory is conducted in a manner that guarantees the sustainability of ecological systems and the fulfilment of ecosystem functions. The question of how precipitation erosion potential dynamics affect crop yields at the regional level remains unanswered. Accordingly, the objective of this study was to identify patterns of spatial and temporal variability of the erosive potential of precipitation and to determine the impact of anthropogenic landscape modification due to agricultural production on soil erosion risks.

Materials and methods

The RUSLE model was employed to estimate annual soil loss. The RUSLE model was developed to predict long-term average annual soil loss. A modern computer interface facilitates the utilisation of RUSLE, whereby physically meaningful input values, widely available in existing databases or easily obtainable from DEM and satellite imagery, are utilised (Kim et al., 2005). The RUSLE model represents the optimal available tool for practical erosion prediction, offering a straightforward approach that can be readily implemented at the local or regional level. Furthermore, numerous parameters, including slope, aspect, and others derived from digital elevation models (DEM) and land use/land cover (LULC) data from satellite imagery, can be readily incorporated into RUSLE (Zerihun et al., 2018). A limitation of the RUSLE model is its inability to route sediment through channels. Consequently, its application is constrained to watersheds of a specific size. Consequently, the model in its original form is not applicable to a very large watershed (Rieke-Zapp & Nearing, 2005). The RUSLE method is applied by representing the basin as a grid of square cells, with the soil erosion calculated for each cell. The RUSLE equation is employed to calculate the anticipated average annual erosion on field slopes (Wischmeier & Smith, 1978):

$$A = R + K + LS + C + P,$$

where the term "A" represents the calculated spatial average soil loss and temporal average soil loss per unit area, expressed in the units selected for "K" and for the specified period selected for "R." In practice, these are typically selected such that A is expressed in tonnes per hectare per year (t/ha*year), R is the rainfall-runoff erosion factor, which is the rainfall erosion rate plus a factor for any significant runoff from snowmelt, expressed in MJ mm/ha*h per year, and K is the soil erosion factor, which is the factor of soil loss per unit of the erosion index for a given soil measured on a standard plot, defined as a 22. The slope length factor (L) is the ratio of soil loss from the length of the field slope to the soil loss from a standard plot measuring 22 m². A 1 m long slope under identical conditions; S is the slope steepness factor, which is the ratio of soil loss from the field slope gradient to the soil loss from a 9% slope under otherwise identical conditions; C is the cover management factor, which is the ratio of soil loss from an area with a given cover and management to soil loss from an identical area under cultivated continuous break; P is the practical support factor, which is the ratio of soil loss with support such as contouring, strip mowing or terracing to soil loss with straight up and down slope farming. The L and S factors represent the non-dimensional effects of slope length and steepness, respectively. The C and P factors represent the non-dimensional effects of cropping and management systems, as well as erosion control practices. In general, the parameters of the RUSLE equation were classified into three categories: erosion susceptibility, erosion sensitivity, and management factors. All of these parameters were derived from geomorphological and precipitation characteristics (Zerihun et al., 2018).

In order to calculate the R factor, our study employed the use of precipitation data spanning a period of 64 years (1960-2023). This data was utilised in accordance with the following equation (Wischmeier & Smith, 1978):

$$R = \sum_{i=1}^{12} 1.735 \times 10^{\left(1.5 log_{10}\left(\frac{P_i^2}{P}\right) - 0.08188\right)}$$

where R is the precipitation erosion factor (MJ mm/ha*h per year); R_i is monthly precipitation (mm); P is annual precipitation (mm).

WorldClim 2, based on a dataset of spatially interpolated monthly climate data for global land areas with a very high spatial resolution (approximately 1 km^2), was used as a spatial sample of precipitation in the study area (Fick & Hijmans, 2017; Cedrez & Hijmans, 2018). The WorldClim 2 raster models were constructed for the period between 1960 and 2023.

The regression dependence of the species was calculated for each administrative district:

$$R = a + b * Y,$$

where R is the precipitation erosion factor, Y is the year from 1960 to 2023, and a and b are the regression coefficients. The regression coefficient b indicates a linear trend in the change of the precipitation erosion factor over time. Linear regression is able to explain a certain part of the variance of the precipitation erosion factor. In the subsequent analysis, we used the residuals of the regression model. The variability of these residuals is also likely to be of a complex nature. The variation in the residuals of the linear regression model contains random noise associated with objective errors in the original data. In addition, a component associated with regular causes of an environmental nature can be expected in the regression residuals.

Prior to the application of principal component analysis, it is essential to address the following question: Has an adequate sample size been obtained for statistical analysis? It is necessary to ascertain whether there is any redundancy between the variables. The suitability of the data set for principal component analysis was evaluated using the Kaiser-Meyer-Olkin (KMO) index. The Kaiser-Meyer-Olkin measure of sample adequacy indicates the proportion of variance in the variables that can be explained by the principal components. Values approaching 1.0 typically indicate the potential utility of factor analysis for empirical data. A value below 0.50 indicates that the results of factor analysis are likely to be of limited utility (Kaiser, 1974). Furthermore, the feasibility of utilising principal component analysis on empirical data can be ascertained through Bartlett's test of sphericity (Bartlett, 1951). The statistically significant number of principal components was parallelised using Horn's analysis (Horn, 1965), which also helped to correct the sampling bias when retaining components. The standard PCA, which assumes that the components are independent of location, should be replaced by Geographically Weighted Principal Components Analysis (GWPCA) in order to account for spatial heterogeneity in the structure of multivariate data (Harris et al., 2011), to account for spatial heterogeneity in the structure of multidimensional data (Lloyd, 2010). In this manner, GWPCA is capable of discerning regions where the assumption of a uniform underlying structure is either inappropriate or overly simplistic. GWPCA is able to estimate two key aspects: firstly, how the effective dimensionality of the data varies in space, and secondly, how the original variables affect each component that varies in space (Fernández et al., 2018).

A Monte Carlo test was employed to ascertain whether the local eigenvalues derived from Geographically Weighted Principal Components Analysis (GWPCA) exhibit significant spatial differences, thereby justifying the utilisation of GWPCA. The pairwise sample locations are successively randomised among the set of data variables. Following each randomisation, the GWPCA is applied, and the standard deviation (SD) of a specific local eigenvalue is calculated. Subsequently, the actual or true standard deviation (SD) of the identical local eigenvalue is incorporated

into the ordered SD distribution. The position of the local eigenvalue within this ranked distribution is indicative of the extent of significant spatial variation (Harris et al., 2011). The time-varying variables (principal components) were subjected to autocorrelation analysis, which identified time lags with statistically significant temporal autocorrelation (Damos, 2016). The cluster analysis was performed in R.

Results

Linear time trend in rainfall erosion variability. The precipitation erosion coefficient exhibited a range of 179.9 ± 114.7 (in 2015) to 616.0 ± 468.9 (in 1974) MJ mm/ha*h per year. The temporal dynamics of this indicator within each administrative district were characterised by a positive or negative trend of changes over time. The upward trend in the overall level of precipitation erosion was typical of the western and north-western regions of the area (Fig. 1).

In the central and eastern regions of the area under study, a downward trend in precipitation erosion was observed over time. The linear trend was found to account for between 0 and 15.3% of the variability in precipitation erosion over time. The most significant linear trend over time was observed in the south-eastern region. For the purposes of further analysis, the time trend was removed from the data set, which was then subjected to further statistical procedures.

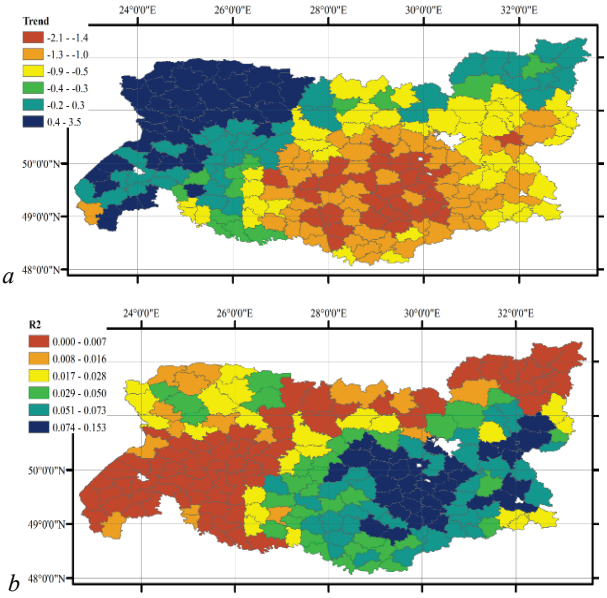

Fig. 1. Spatial variation of the temporal linear trend of precipitation erosion factor variability (*a*) and the coefficient of determination of the temporal linear model (*b*)

Global principal component analysis. The variability of the precipitation erosion factor was investigated for 203 administrative districts for 64 variables (years). Since the KMO is 0.16, according to Kaiser's rule of thumb, the data should be considered not very suitable for principal component analysis. Nevertheless, Bartlett's test of sphericity ($P < 0.05$) indicates that principal component analysis can be applied to such data. The global principal component analysis identified 5 statistically significant principal components that together were able to explain 84.8% of the variation in the detrended rainfall erosion data (Table 1).

Table 1
Results of the global principal component analysis

Principal component	Adjusted eigenvalue*	Eigenvalue	Shift	Variation explained	Standard deviation
1	20.35	21.66	1.31	20.35	4.68
2	14.54	15.73	1.19	14.54	3.47
3	9.06	10.16	1.10	9.06	3.27
4	4.47	5.49	1.02	4.47	2.16
5	2.40	3.35	0.95	2.40	1.73

Notes: * – according to the Horn procedure.

Years of research in the principal component space form certain patterns. The properties of the principal components can be better understood by presenting their variability in time (Fig. 2) and space (Fig. 3). All of the principal components contrast a particular sequence of years with another sequence of years in terms of rainfall erosion, which has a certain spatial structure. Principal component 1 is the most sensitive to the fluctuations in rainfall erosion variability with periods of 1, 5, and 11 years (Fig. 3). This principal component contrasts the northeastern part of the region with its western part (Fig. 2). Principal component 1 is positively correlated with clay and silt content in the soil, and negatively correlated with sand content (Table 2). The values of this principal component are higher in those landscapes where the proportion of broadleaf forests and meadows is higher and the proportion of agricultural areas is lower.

Principal component 2 is sensitive to the variability components with periods of 3, 7 and 9 years. This principal component assigns the southwestern part to all other areas. Principal component 2 is positively correlated with soil organic matter and sand, but negatively correlated with clay and silt. Higher values of this principal component are found in landscapes with a higher proportion of coniferous, broadleaved or mixed forests, but a lower proportion of agricultural areas or sparse vegetation.

Principal component 3 is sensitive to variability components with periods of 4, 7 and 14 years. It contrasts the dynamics of fluctuations in the northwest and southeast of the region. Principal component 3 is positively correlated with soil organic carbon and sand content and negatively correlated with clay and silt content. Higher values of this principal component are found in landscapes with a higher proportion of coniferous, broadleaf or mixed forests, but a lower proportion of agricultural areas or sparse vegetation.

Principal component 4 is sensitive to the components of variability with periods of 5, 10 and 14 years. It contrasts the dynamics of oscillatory processes in the centre with those in the north of the region and other areas. Principal component 4 is positively correlated with clay content and negatively correlated with soil organic carbon and sand content. This component is positively correlated with the proportion of rainfed land or grass or sparse vegetation cover and negatively correlated with the proportion of broadleaf, coniferous or mixed forests.

Principal component 5 is sensitive to variability components with periods that are multiples of 2 years: an increase in precipitation erosion in the following year is accompanied by a decrease in precipitation erosion the year after. It contrasts the dynamics of oscillatory processes in the centre of the region and in other areas. Principal component 5 is negatively correlated with organic carbon content. This component is negatively correlated with the proportion of agricultural land and the mosaic of vegetation of different origin and agricultural land.

Geographically weighted principal component analysis. The Monte Carlo test was conducted with the objective of determining whether the eigenvalues of the data matrix are characterised by a spatial component of variation. The level of significance for testing the standard deviation of the local eigenvalues derived from the GWPCA results is 0.01. This value indicates that the hypothesis of spatial invariance of the local eigenvalues can be statistically significantly rejected. Alternatively, it may be interpreted as evidence of a high level of spatial non-stationarity present in the rainfall erosivity factor data.

A decision must be made regarding the number of principal components to be retained prior to identifying the optimal pass-through window. The preliminary global principal component analysis indicates that the first two components together can explain 55.0% of the variation in the data structure. It is therefore reasonable to retain the two components for further GWPCA processing. In the process of selecting an adaptive window, the optimal window of 220 nearest neighbours was established and selected for the GWPCA procedure. In order to obtain the corresponding results of the global principal component analysis, only the first two principal components (GWPC 1 and GWPC 2) were interpreted for comparison purposes.

The results of the GWPCA procedure can be visualised and interpreted by focusing on two key aspects: firstly, how the dimensionality of the data varies spatially, and secondly, how the original variables influence the principal components. The proportion of spatial variation in the total variation is observed to exhibit a notable degree of variability, with the formati-

on of spatially homogeneous clusters in the meridional direction (Fig. 4). In comparison to a global principal component analysis, the GWPCA method has been demonstrated to be an efficient and effective approach for analysing the spatial patterns of regional precipitation erosion distributions, through the mapping of the spatial variability of principal components.

Two homogeneous clusters were identified based on the results of the GWPC 1 cluster analysis (Fig. 5). These clusters divide the study area into two zones: eastern and western. Cluster 1, which occupies the eastern part of the region, is characterised by an oscillatory process with autocorrelation with a lag of 2, 6 and 8 years (Fig. 6). Cluster 2 covers the western part of the territory and is characterised by an oscillatory process with a lag of 5, 10 and 13 years. The phase spectrum indicates that the oscillatory processes in clusters 1 and 2 are related and are the result of a phase shift with a lag that corresponds to the most important autocorrelation processes. Three homogenous clusters were identified based on the results of the GWPC 2 cluster analysis (Fig. 5). These clusters divide the study area into three zones: eastern, western and northern intercalary. Cluster 1, which occupies the eastern part of the region, is characterised by an oscillatory process with autocorrelation with lags of 2, 6 and 8 years (Fig. 7). Cluster 2 covers the western part of the territory and is characterised by an oscillatory process with a lag of 5, 10 and 13 years. The phase spectrum indicates that the oscillatory processes in clusters 1 and 2 are related and are the result of a phase shift with a lag that corresponds to the most important autocorrelation processes.

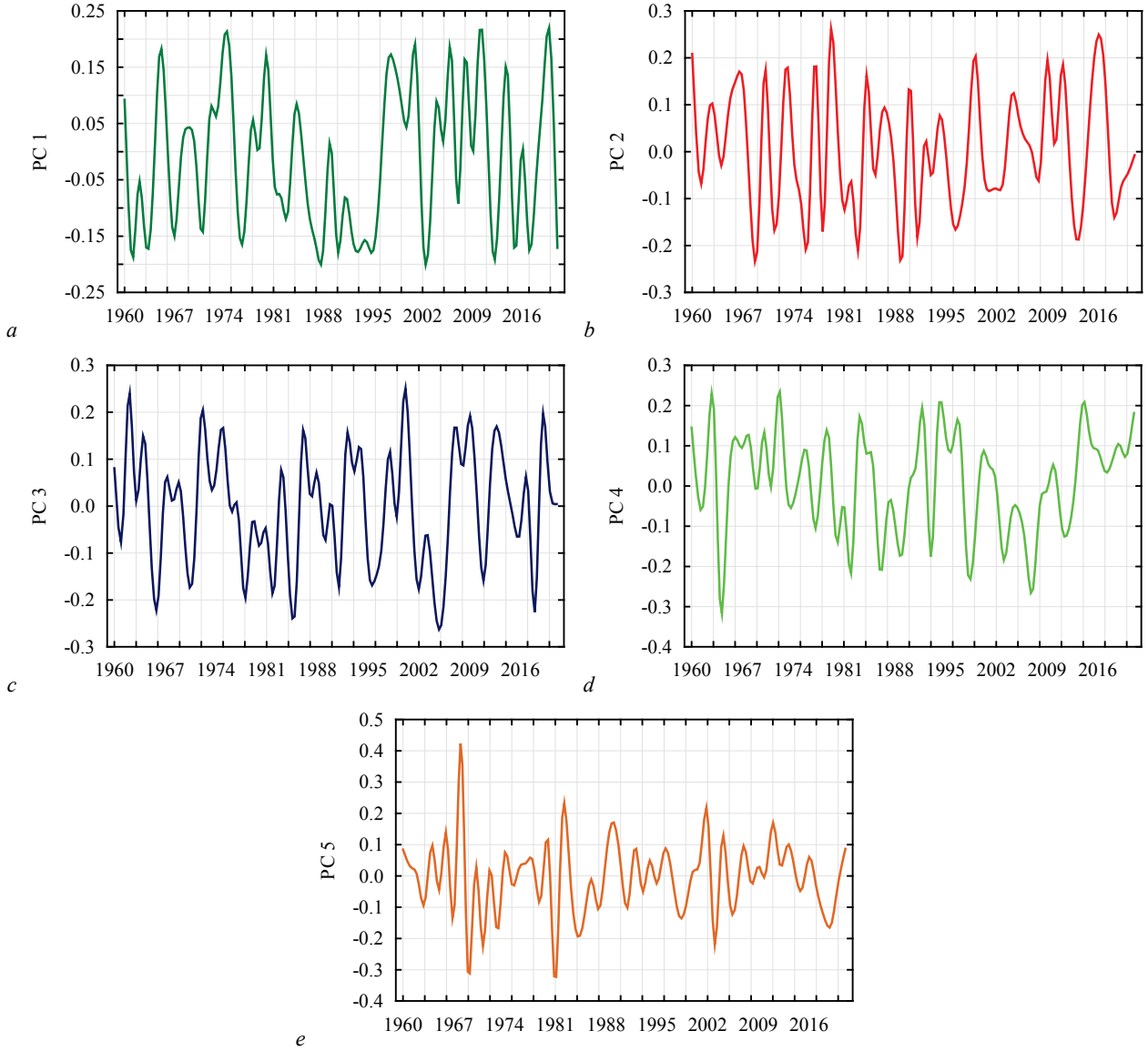

Fig. 2. Time variation of the loadings of principal components 1–5: *a* is the principal component 1 (autocorrelation 0.14 ± 0.09 for lag 1, 0.10 ± 0.09 for lag 5 and –0.23 ± 0.11 for lag 11), *b* is the principal component 2 (autocorrelation –0.20 ± 0.12 for lag 3, 0.28 ± 0.12 for lag 7 and –0.21 ± 0. 12 for lag 9), *c* is the principal component 3 (autocorrelation –0.18 ± 0.09 for lag 4, 0.12 ± 0.09 for lag 7 and 0.13 ± 0.11 for lag 14), *d* is the principal component 4 (autocorrelation –0. 18 ± 0.09 for lag 5, –0.19 ± 0.09 for lag 10 and –0.24 ± 0.11 for lag 14), *e* is the principal component 5 (autocorrelation –0.40 ± 0.12 for lag 1 and 0.26 ± 0.12 for lag 2)

Discussion

Rainfall represents a significant contributing factor to soil erosion (Panagos et al., 2015). The impact of water erosion on soil quality and productivity is multifaceted. It can be observed that water erosion reduces the infiltration rate, water holding capacity, nutrient content, organic matter, soil biota and soil thickness (Pimentel et al., 1995). The effect of the kinetic energy of a raindrop impact and the rate of runoff on soil erosion is quantified by the rainfall erosivity factor (R-factor), which is dependent on both the total amount of precipitation that falls during the year and its redistribution during the year. The estimated value of the R-factor within the study area is lower than the EU average, which is 722 MJ mm/ha*h per year (Panagos et al., 2015). The estimated value falls within the range of variation that is typical of the Boreal and Continental biogeographic regions. The Boreal region has an estimated value of 359.5 MJ mm/ha*h per year, while the Continental region has an estimated value of 695.7 MJ mm/ha*h per year. The R-factor, or rainfall erosivity, is a pivotal parameter for evaluating soil erosion losses and soil erosion risk. The occurrence

of extreme rainfall and high erosion can result in a reduction or even the complete destruction of the yield of perennial crops.

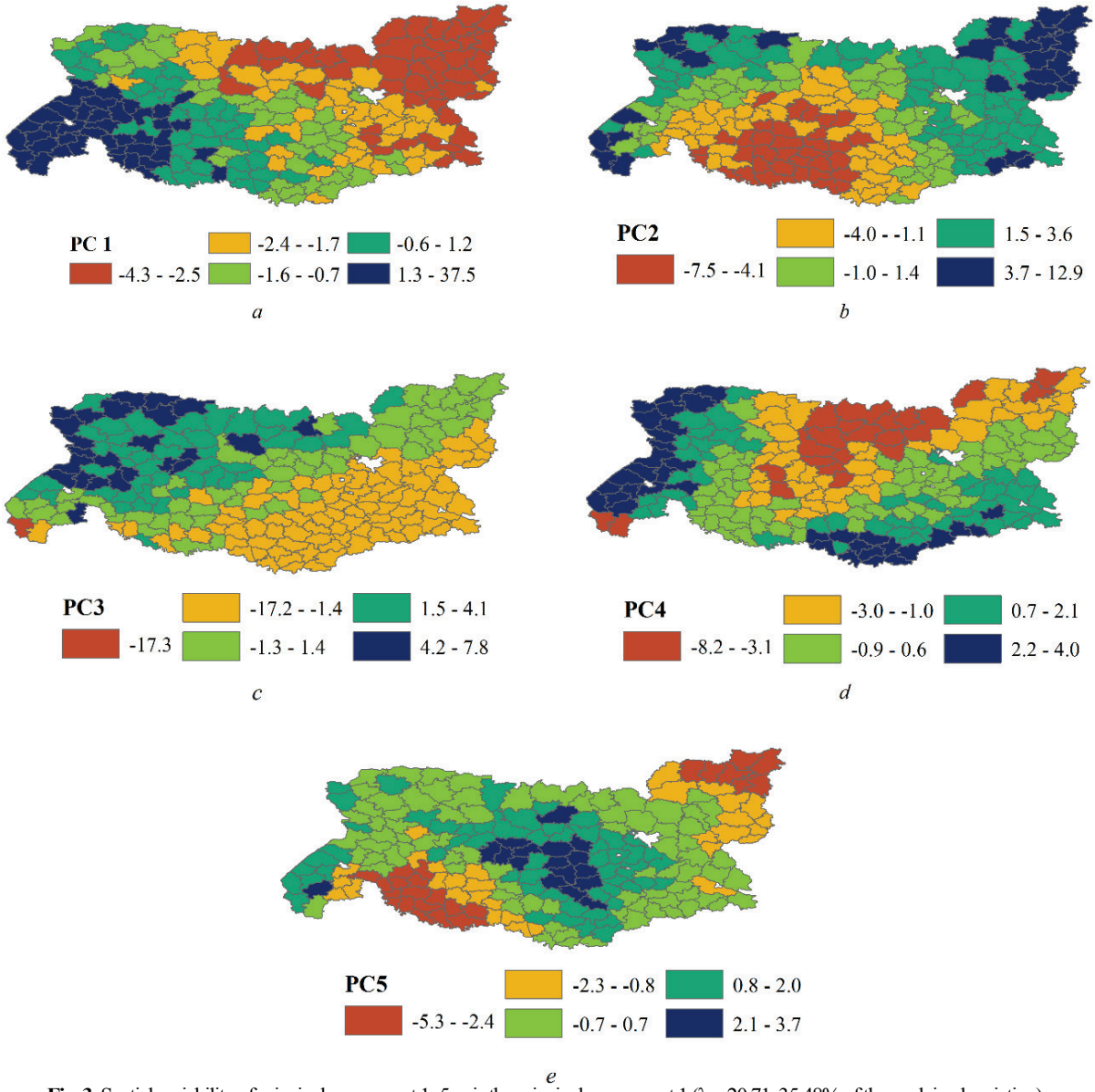

Fig. 3. Spatial variability of principal component 1–5: *a* is the principal component 1 (λ = 20.71, 35.48% of the explained variation), *b* is the principal component 2 (λ = 10.97, 19.56% of the explained variation), *c* is the principal component 3 (λ = 9.69, 17.35% of the explained variation), *d* is the principal component 4 (λ = 3.68, 7.53% of the explained variation), e is the principal component 5 (λ = 2.07, 4.84% of the explained variation)

Table 2

Correlation between principal components and ecological properties of the territories (correlation coefficients are statistically significant for $P < 0.05$)

	Variables	Principal components				
		PC 1	PC 2	PC 3	PC 4	PC 5
Soil properties	Organic matter	–	0.67	0.16	–0.36	–0.32
	Clay	0.15	–0.52	–0.52	0.35	–
	Sand	–0.15	0.54	0.44	–0.21	–
	Silt	0.14	–0.54	–0.29	–	–
Types of land-scape cover (Glob-Cover)	Rainfed croplands	–	–0.52	–0.35	0.35	–
	Mosaic Croplands (50–70%) / Vegetation (grassland/shrubland/forest) (20–50%)	–0.44	–0.23	–0.14	–	–0.18
	Mosaic vegetation (grassland/ shrubland/ forest) (50–70%) / cropland (20–50%)	0.29	–	–0.55	–	–0.19
	Closed (>40%) broad-leaved deciduous forest (>5m)	0.32	0.31	0.41	–	–
	Closed (>40%) needle-leaved evergreen forest (>5m)	–	0.29	0.19	–0.43	–
	Open (15–40%) needle-leaved deciduous or evergreen forest (>5m)	–	0.44	0.25	–0.35	–
	Closed to open (>15%) mixed broad-leaved and needle-leaved forest (>5m)	–	0.41	0.33	–0.40	–
	Mosaic grassland (50–70%) / forest or shrubland (20–50%)	0.54	–	–	0.26	–
	Closed to open (>15%) herbaceous vegetation (grassland, savannas or lichens/mosses)	0.40	–	–	0.15	–
	Sparse (<15%) vegetation	–	–0.26	–0.42	0.27	–
	Closed to open (>15%) grassland or woody vegetation on regularly flooded or waterlogged soil – Fresh, brackish or saline water	–	–	–	–	–
	Artificial surfaces and associated areas (Urban areas >50%)	–	–	–	–	–
	Water bodies	–	–	–	–	–

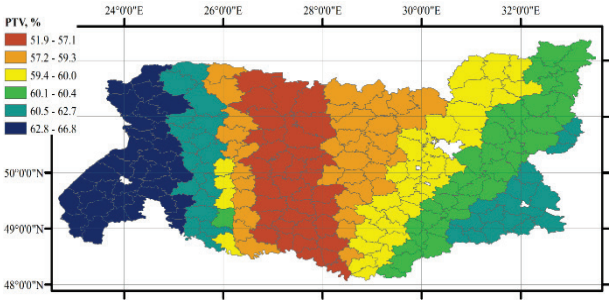

Fig. 4. Spatial variation of the percentage of total variation (PTV) of the first two principal components

An understanding of the spatial and temporal dynamics of the R-factor is of great importance for the formulation of crop rotation plans, the implementation of agricultural management strategies and the development of conservation policies (Renschler et al., 1999). In Europe, the annual pattern of the R-factor from 1961 to 2018 exhibited a positive trend in 15% of cases and a negative trend in 7% of cases (Bezak et al., 2020). The study area is subdivided into two zones, one exhibiting an increase in erosion over time and the other a decrease. The increase in precipitation erosion was observed in the north-western and western regions of the area. This zone encompasses Polissya and the foothills of the Carpathian region. It is evident that the soils in this zone are highly susceptible to erosion processes. The soils of Polissya are predominantly sandy and exhibit a diminished capacity to resist water erosion. The topographical characteristics of Prykarpattia contribute to an elevated risk of erosion, largely due to the prevalence of steep inclines. The downward trend in the water erosion factor is evident in the central and south-eastern regions of the area. This trend should be regarded as beneficial, given that this is the area where a significant proportion of the region's productive agricultural land is concentrated. It is important to note, however, that the coefficients of determination of the respective linear models on which the trend was calculated are relatively low, indicating that other factors play a more significant role in explaining the spatial and temporal patterns of variation of the erosion factor.

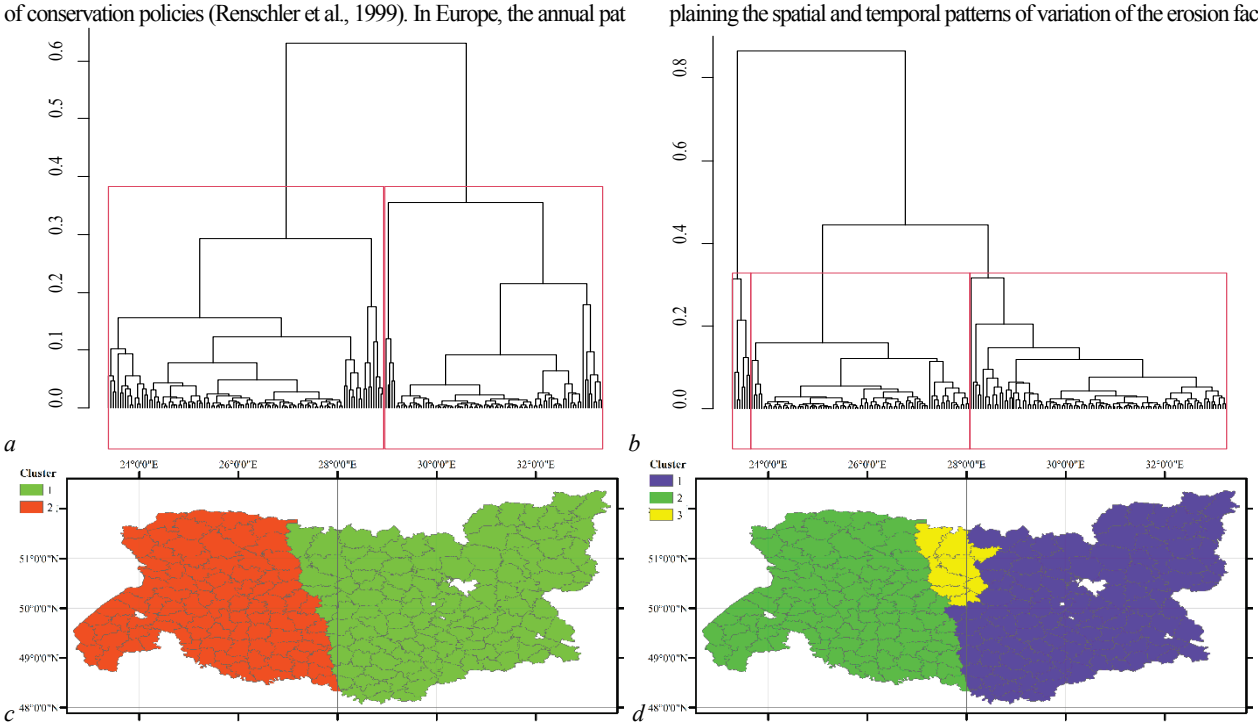

Fig. 5. Cluster analysis of administrative districts by the values of factor loadings GWPC 1 (*a*) and GWPC 2 (*b*) and spatial position of clusters obtained on the basis of factor loadings GWPC 1 (*c*) and GWPC 2 (*d*)

Two distinct approaches have been employed in sequence to elucidate the spatial and temporal dynamics of variability in erosion factors. These comprise traditional principal component analysis and spatially weighted principal component analysis. The traditional principal component analysis is predicated on the assumption that the covariance structure between variables remains constant across the entire territory (Yorkina et al., 2022). This approach is referred to as global principal component analysis. The spatially weighted principal component analysis posits that the covariance structure varies in a spatially explicit manner, whereby zones of smaller spatial coverage can be identified where such structures are constant. The extracted principal components indicated the presence of oscillatory time trends, characterised by varying frequency characteristics. The linear trend was found to account for between 0 and 15.3% of the observed variation in rainfall erosion. In contrast, the principal components collectively explained 84.8% of the variation, with the geographically weighted approach accounting for an even greater proportion. This suggests that oscillatory dynamics, rather than a linear trend, play a significant role in shaping patterns of rainfall erosion variability. It is similarly conceivable that the observed linear trend constitutes merely a component of an oscillatory process, with a considerably longer period of fluctuation than that encompassed by the time frame of the present study.

The spatial patterns of the principal components of higher ordinal numbers can be explained by the influence of the geographical continentality factor (Kunakh & Zhukov, 2024). The variation in precipitation levels and the seasonal dynamics of precipitation in the west-east direction give rise to patterns that differentiate the study area into regions that can be effectively compared with the eastern and western zones of the region. The principal components with lower ordinal numbers describe a more detailed spatial structure, which can be explained by the specific landscape cover of the respective areas. Principal components 1 and 2 are correlated with environmental markers that exhibit a zonal or sectoral geographical distribution. In fact, they can be considered covariates that indicate the geographical zonality of the region's environmental conditions. These include the ratio of sand to clay and silt, as well as the proportion of forest and agricultural land. Polissia is distinguished by soils with a relatively high sand content, which often render them unsuitable for agricultural use. Consequently, these regions retain a relatively dense forest cover. The southern and eastern regions are typified by soil types with a grain size distribution that is conducive to enhanced agricultural productivity. This often coincides with the clearance of forest cover (Kunakh et al., 2021). The precipitation fluctuations that generate the patterns identified by principal components 3–5 can be induced by the influence of different types of land cover. To illustrate, the pattern identified by principal component 3 can be attributed to the contrasting dynamics of the proportion of herbaceous vegetation and broadleaf forests.

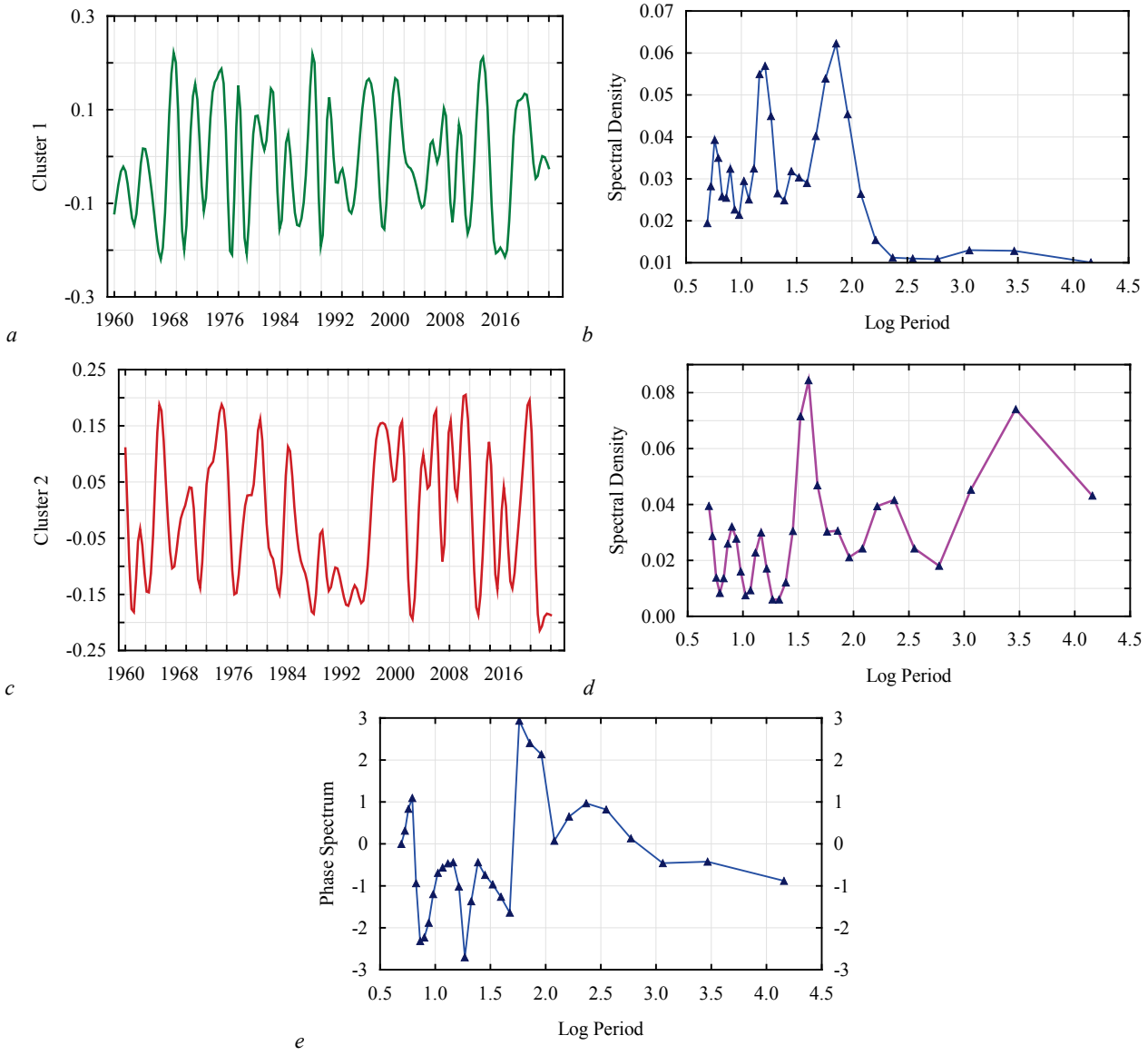

Fig. 6. Temporal variation of the loadings of the principal component GWPC 1 for clusters 1 and 2: *a* is the cluster 1 (autocorrelation –0.18 ± 0.12 for lag 2, 0.15 ± 0.11 for lag 6 and 0.15 ± 0.11 for lag 8), *b* is the spectral density of the oscillatory process for cluster 1, *c* is the cluster 2 (autocorrelation 0.18 ± 0.11 for lag 5, 0.17 ± 0.11 for lag 10, and –0.21 ± 0.11 for lag 13), *d* is the spectral density of the oscillatory process for cluster 2; *e* is the phase spectrum of oscillatory processes within clusters 1 and 2

Broadleaf forests exert a considerable influence on the interaction between the atmosphere and the Earth's surface, which has a marked impact on the evaporation of moisture from the Earth's surface and the amount of precipitation (Koshelev et al., 2021). This provides an explanation for the formation of patterns of variability in the precipitation erosion factor, which is consistent with the level of forest cover (Mykhailyuk et al., 2023). The influence of coniferous vegetation gives rise to Factor 4, while Factor 5 is induced by the influence of herbaceous vegetation. It is also important to consider the significant impact of agricultural land on the formation of spatial patterns of erosion factor variability. This influence may be the result of a formal correlation between the variability of agricultural land in different biogeographical zones. To illustrate, components 1 and 2 are associated with the geographical heterogeneity of the region, which also gives rise to variability in the level of agricultural development. In Polissya, this phenomenon is less pronounced, whereas in the Forest-Steppe, it is particularly noteworthy. It is not possible to exclude the possibility that different vegetation types contribute to the formation of large-scale patterns of the precipitation erosion factor. However, this conclusion cannot be reached on formal grounds.

The generation of temporal patterns of precipitation erosion, which also have a spatial context, can be explained by the influence of periodic changes in the state of the Earth's vegetation cover. It is also possible that the reverse effect, whereby the intensity of erosion processes affects the state of vegetation, may be a contributing factor. It can be posited that the impact of erosion processes is particularly significant in relation to agricultural land, which constitutes a considerable proportion of the region's landscape. The rhythm of precipitation determines the impact of erosion and can also affect the condition of phytophagous animals, which can significantly affect the condition of both agricultural plants and forest ecosystems. The occurrence of large-scale infestations of wood-boring pests can result in the defoliation of trees in forest ecosystems. This phenomenon has the potential to influence both the rate of evaporation from the Earth's surface and the susceptibility of soil surfaces to erosion.

Conclusion

The precipitation erosivity coefficient exhibited considerable variation, ranging from 179.9 ± 114.7 to 616.0 ± 468.9 MJ mm/ha*h per year, in the Polissya and Forest-Steppe zones of Ukraine from 1960 to 1923. The linear trend was found to account for between 0 and 15.3% of the variability in precipitation erosion over time. The upward trend in the overall level of precipitation erosion was a typical feature of the western and northwestern regions of the area. In the central and eastern regions of the area, there was a decline in the incidence of rainfall erosion over time.

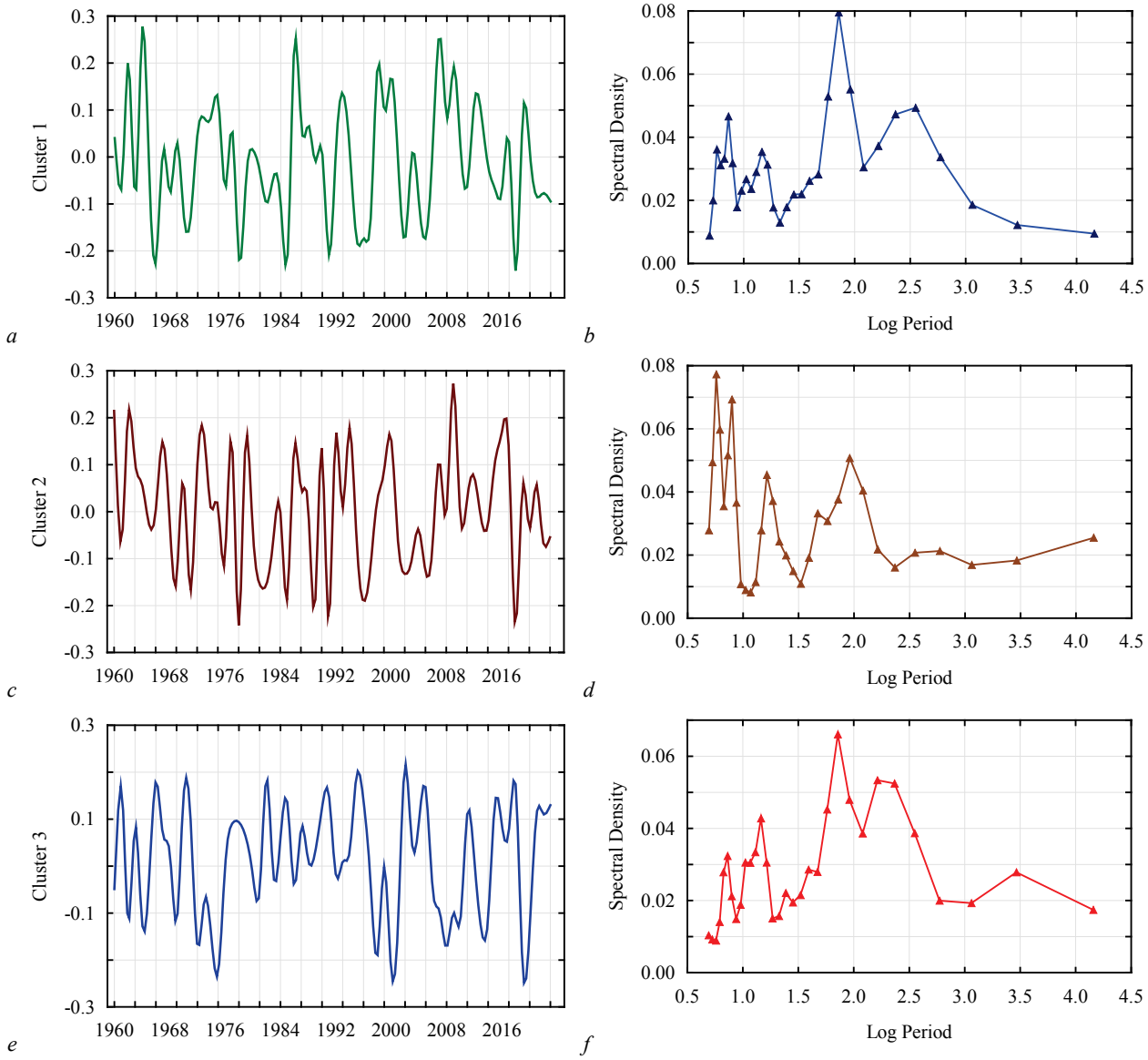

Fig. 7. Temporal variation of the GWPC 2 principal component loads for clusters 1, 2, and 3: *a* is the cluster 1 (autocorrelation –0.21 ± 0.12 for lag 4 and 0.21 ± 0.11 for lag 13), *b* is the spectral density of the oscillatory process for cluster 1, *c* is the cluster 2 (autocorrelation –0.19 ± 0.11 for lag 3 and 0.18 ± 0.11 for lag 7), *d* is the spectral density of the oscillatory process for cluster 2; *e* – cluster 3 (autocorrelation –0.25 ± 0.11 for lag 4 and 0.11 ± 0.09 for lag 12), *f* is the spectral density of the oscillatory process for cluster 3

A global principal component analysis enabled the identification of five statistically significant principal components, which collectively explained 84.8% of the variation in the detrended rainfall erosion data. The spatial patterns of principal components with higher ordinal numbers can be explained by the influence of the geographical continentality factor. The principal components with lower ordinal numbers characterise a more detailed spatial structure and can be explained by the peculiarities of the landscape cover of the respective territories. It should also be noted that agricultural land plays an important role in the formation of spatial patterns of erosion factor variability. The generation of temporal patterns of the precipitation erosion factor, which also have a spatial context, can be explained by the influence of periodic changes in the state of the Earth's vegetation cover.

References

Bartlett, M. S. (1951). The effect of standardization on a χ^2 approximation in factor analysis. Biometrika, 38(3/4), 337.

Bezak, N., Ballabio, C., Mikoš, M., Petan, S., Borrelli, P., & Panagos, P. (2020). Reconstruction of past rainfall erosivity and trend detection based on the REDES database and reanalysis rainfall. Journal of Hydrology, 590, 125372.

Cedrez, C. B., & Hijmans, R. J. (2018). Methods for spatial prediction of crop yield potential. Agronomy Journal, 110(6), 2322–2330.

Christensen, O., Yang, S., Boberg, F., Fox Maule, C., Thejll, P., Olesen, M., Drews, M., Sørup, H., & Christensen, J. (2015). Scalability of regional climate change in Europe for high-end scenarios. Climate Research, 64(1), 25–38.

Cook, H. L. (1937). The nature and controlling variables of the water erosion process. Soil Science Society of America Journal, 1(C), 487–494.

Damos, P. (2016). A stepwise algorithm to detect significant time lags in ecological time series in terms of autocorrelation functions and ARMA model optimisation of pest population seasonal outbreaks. Stochastic Environmental Research and Risk Assessment, 30(7), 1961–1980.

Dash, S. S., & Maity, R. (2023). Effect of climate change on soil erosion indicates a dominance of rainfall over LULC changes. Journal of Hydrology: Regional Studies, 47, 101373.

Fernández, S., Cotos-Yáñez, T., Roca-Pardiñas, J., & Ordóñez, C. (2018). Geographically weighted principal components analysis to assess diffuse pollution sources of soil heavy metal: Application to rough mountain areas in Northwest Spain. Geoderma, 311, 120–129.

Fick, S. E., & Hijmans, R. J. (2017). WorldClim 2: New 1-km spatial resolution climate surfaces for global land areas. International Journal of Climatology, 37(12), 4302–4315.

Gámez-Balmaceda, E., López-Ramos, A., Martínez-Acosta, L., Medrano-Barboza, J. P., Remolina López, J. F., Seingier, G., Daesslé, L. W., & López-Lambraño, A. A. (2020). Rainfall intensity-duration-frequency relationship. case study: Depth-duration ratio in a semi-arid zone in Mexico. Hydrology, 7(4), 78.

Ganasri, B. P., & Ramesh, H. (2016). Assessment of soil erosion by RUSLE model using remote sensing and GIS – A case study of Nethravathi Basin. Geoscience Frontiers, 7(6), 953–961.
Harris, P., Brunsdon, C., & Charlton, M. (2011). Geographically weighted principal components analysis. International Journal of Geographical Information Science, 25(10), 1717–1736.
Horn, J. L. (1965). A rationale and test for the number of factors in factor analysis. Psychometrika, 30(2), 179–185.
Kaiser, H. F. (1974). An index of factorial simplicity. Psychometrika, 39(1), 31–36.
Kim, J. B., Saunders, P., & Finn, J. T. (2005). Rapid assessment of soil erosion in the Rio Lempa Basin, Central America, using the universal soil loss equation and geographic information systems. Environmental Management, 36(6), 872–885.
Koshelev, O., Koshelev, V., Fedushko, M., & Zhukov, O. (2021). Annual course of temperature and precipitation as proximal predictors of birds' responses to climatic changes on the species and community level. Folia Oecologica, 48(2), 118–135.
Kunakh, O. M., Yorkina, N. V., Turovtseva, N. M., Bredikhina, J. L., Balyuk, J. O., & Golovnya, A. V. (2021). Effect of urban park reconstruction on physical soil properties. Ecologia Balkanica, 13(2), 57–73.
Kunakh, O., & Zhukov, O. (2024). Spatial organization of the soil macrofauna community of an oak forest in the steppe zone of Ukraine. Studia Biologica, 18(3), 99–120.
Lloyd, C. D. (2010). Analysing population characteristics using geographically weighted principal components analysis: A case study of Northern Ireland in 2001. Computers, Environment and Urban Systems, 34(5), 389–399.
Majewski, M., & Szpikowski, J. (2024). Effect of rainfall parameters on soil erosion in Chwalimski Brook catchment, NW Poland. Geomorphology, 454, 109167.
Mykhailyuk, T., Lisovets, O., & Tutova, H. (2023). Steppe vegetation islands in the gully landscape system: Hemeroby, naturalness and phytoindication of ecological regimes. Regulatory Mechanisms in Biosystems, 14(4), 581–594.
Nearing, M. A. (2001). Potential changes in rainfall erosivity in the US with climate change during the 21st century. Journal of Soil and Water Conservation, 56, 229–232.
Nearing, M. A., Yin, S. Q., Borrelli, P., & Polyakov, V. O. (2017). Rainfall erosivity: An historical review. Catena, 157, 357–362.
Panagos, P., Ballabio, C., Borrelli, P., Meusburger, K., Klik, A., Rousseva, S., Tadić, M. P., Michaelides, S., Hrabalíková, M., Olsen, P., Aalto, J., Lakatos, M., Rymszewicz, A., Dumitrescu, A., Beguería, S., & Alewell, C. (2015). Rainfall erosivity in Europe. Science of the Total Environment, 511, 801–814.
Panagos, P., Ballabio, C., Meusburger, K., Spinoni, J., Alewell, C., & Borrelli, P. (2017). Towards estimates of future rainfall erosivity in Europe based on REDES and WorldClim datasets. Journal of Hydrology, 548, 251–262.
Pandey, S., Kumar, P., Zlatic, M., Nautiyal, R., & Panwar, V. P. (2021). Recent advances in assessment of soil erosion vulnerability in a watershed. International Soil and Water Conservation Research, 9(3), 305–318.
Pimentel, D., Harvey, C., Resosudarmo, P., Sinclair, K., Kurz, D., McNair, M., Crist, S., Shpritz, L., Fitton, L., Saffouri, R., & Blair, R. (1995). Environmental and economic costs of soil erosion and conservation benefits. Science, 267(5201), 1117–1123.
Renard, K. G., & Freimund, J. R. (1994). Using monthly precipitation data to estimate the R-factor in the revised USLE. Journal of Hydrology, 157(1–4), 287–306.
Renschler, C. S., Mannaerts, C., & Diekkrüger, B. (1999). Evaluating spatial and temporal variability in soil erosion risk – rainfall erosivity and soil loss ratios in Andalusia, Spain. Catena, 34(3–4), 209–225.
Rieke-Zapp, D. H., & Nearing, M. A. (2005). Digital close range photogrammetry for measurement of soil erosion. Photogrammetric Record, 20(109), 69–87.
Shiono, T., Ogawa, S., Miyamoto, T., & Kameyama, K. (2013). Expected impacts of climate change on rainfall erosivity of farmlands in Japan. Ecological Engineering, 61, 678–689.
Westra, S., Fowler, H. J., Evans, J. P., Alexander, L. V., Berg, P., Johnson, F., Kendon, E. J., Lenderink, G., & Roberts, N. M. (2014). Future changes to the intensity and frequency of short-duration extreme rainfall. Reviews of Geophysics, 52(3), 522–555.
Wischmeier, W. H., & Smith, D. D. (1978). Predicting rainfall erosion loss: A guide to conservation planning. Agricultural Handbook No. 537. US Department of Agriculture – Agricultural Research Service.
Yakovenko, V., Kunakh, O., Tutova, H., & Zhukov, O. (2023). Diversity of soils in the Dnipro River valley (based on the example of the Dnipro-Orilsky Nature Reserve). Folia Oecologica, 50(2), 119–133.
Yorkina, N., Goncharenko, I., Lisovets, O., & Zhukov, O. (2022). Assessment of naturalness: The response of social behavior types of plants to anthropogenic impact. Ekológia (Bratislava), 41(2), 135–146.
Zerihun, M., Mohammedyasin, M. S., Sewnet, D., Adem, A. A., & Lakew, M. (2018). Assessment of soil erosion using RUSLE, GIS and remote sensing in NW Ethiopia. Geoderma Regional, 12, 83–90.
Zymaroieva, A., Zhukov, O., Fedoniuk, T., Pinkina, T., & Hurelia, V. (2021). The relationship between landscape diversity and crops productivity: Landscape scale study. Journal of Landscape Ecology, 14(1), 39–58.